



Cytotoxic activity and potential estrogen receptor interactions of extracts from red ginger endophytic fungus *Aspergillus niger* ZOBT1

Herland Satriawan¹, Putri Ulinza², Ping-Chung Kuo¹, Dian Handayani^{2*}

¹School of Pharmacy, College of Medicine, National Cheng Kung University, Tainan, Taiwan.

²Sumatran Biota Laboratory/Faculty of Pharmacy, Universitas Andalas, Padang, Indonesia.

ARTICLE HISTORY

Received on: 17/10/2025
Accepted on: 02/02/2026
Available Online: 05/03/2026

Key words:

Zingiber officinale Roscoe var. rubrum, fonsecinone A, cytotoxicity, molecular docking, natural anticancer agent.

ABSTRACT

Cancer remains a major global health challenge, driving the search for novel anticancer agents from natural sources. Endophytic fungi associated with medicinal plants, particularly red ginger (*Zingiber officinale* Roscoe var. rubrum), represent promising reservoirs of bioactive metabolites with cytotoxic potential. In this study, the cytotoxic activity of ethyl acetate extracts obtained from endophytic fungi isolated from red ginger was evaluated. Preliminary screening using the brine shrimp lethality test identified potent extracts with lethal concentration values below 100 ppm. These active extracts were subsequently assessed for cytotoxicity against the human breast cancer cell line Michigan Cancer Foundation-7 using the 3-(4,5-dimethylthiazol-2-yl)-2,5-diphenyl tetrazolium bromide assay. Among the tested isolates, ZOBT1 exhibited notable cytotoxicity, with an inhibitory concentration value of 20.103 µg/ml. Molecular characterization confirmed the fungal isolate as *Aspergillus niger* ZOBT1. Furthermore, molecular docking analysis revealed that Fonsecinone A, a compound derived from this isolate, demonstrated stable interactions with key residues at the estrogen receptor (ER) binding site. Specifically, Fonsecinone A interacted with Trp393, a residue adjacent to the canonical ER binding site, yielding a docking score of -5.3536 kcal/mol and a root mean square deviation_refine of 1.7373 Å, suggesting a plausible mechanism for its anticancer activity. Overall, these findings highlight the potential of red ginger-associated endophytic fungi as promising sources of bioactive metabolites with anticancer properties, emphasizing the need for further pharmacological and mechanistic studies to validate their therapeutic relevance.

1. INTRODUCTION

Cancer remains one of the leading causes of mortality worldwide, with approximately 20 million new cases and 9.7 million deaths reported in 2022 alone [1]. Despite remarkable advances in medical science, cancer treatment continues to encounter significant challenges, including drug resistance [2], severe side effects [3], and high treatment costs [4]. These limitations underscore the urgent need to explore alternative and complementary therapeutic strategies. Medicinal plants, rich in diverse bioactive compounds, have long been pivotal in

the discovery and development of drugs for various diseases, including cancer [5,6].

Red ginger (*Zingiber officinale* Roscoe var. rubrum) has traditionally been valued in Asian medicine for its therapeutic properties. It is known to reduce inflammation, combat oxidative stress, relieve pain, and exhibit anticancer potential [7-9]. These benefits are primarily attributed to the major constituents of ginger, namely gingerols, shogaols, and zingerone, which have been shown to inhibit cancer cell proliferation and induce apoptosis in several cancer cell lines [10]. Building upon this pharmacological foundation, greater attention is now being directed toward the endophytic fungi associated with red ginger, as they may represent untapped sources of bioactive metabolites with therapeutic relevance.

Endophytic fungi are microorganisms that colonize internal plant tissues without inducing disease symptoms, forming symbiotic associations. These fungi enhance the host

*Corresponding Author

Dian Handayani, Sumatran Biota Laboratory/Faculty of Pharmacy,
Universitas Andalas, Padang, Indonesia.

E-mail: dianhandayani@phar.unand.ac.id

plant's resilience to environmental stresses and protect against pathogenic attacks [11,12]. Beyond their ecological role, endophytic fungi have attracted considerable interest as prolific producers of bioactive secondary metabolites with applications in pharmaceuticals, agriculture, and biotechnology [13,14]. Notably, endophytes associated with medicinal plants have been reported to synthesize compounds with strong anticancer properties, positioning them as valuable candidates for natural product-based drug discovery [15-17].

Previous investigations identified 11 distinct endophytic fungi from red ginger, several of which demonstrated potent antibacterial activity in screening assays [18]. Building on these findings, the present study focuses on exploring the anticancer potential of these fungal isolates. Ethyl acetate extracts from the identified endophytes were initially screened using the brine shrimp lethality test (BSLT), with extracts showing lethal concentration (LC_{50}) values below 100 ppm considered bioactive and selected for further testing. These extracts were subsequently evaluated for cytotoxicity against the human breast cancer cell line Michigan Cancer Foundation-7 (MCF-7) using the 3-(4,5-dimethylthiazol-2-yl)-2,5-diphenyl tetrazolium bromide (MTT) assay. The MCF-7 line was chosen as it is one of the most widely used models for estrogen receptor (ER)-positive breast cancer, which accounts for approximately 70% of hormone-dependent breast cancer cases [19]. Accordingly, estrogen receptor alpha ($ER\alpha$) was selected as the molecular docking target to provide a focused evaluation of Fonsecinone A, while recognizing that future work will expand to additional cancer cell lines and molecular targets for broader validation.

To complement the biological assays, molecular docking analyses were performed to elucidate the interaction of bioactive metabolites with cancer-related target proteins. These analyses provided insights into binding affinities, reflecting the strength and binding orientations of the interactions, and described how the compounds fit within the receptor's active site. Such molecular-level insights are essential for understanding the potential mechanisms underlying cytotoxic activity and

identifying promising lead compounds [20-22]. For validation, Raloxifene, a clinically approved selective estrogen receptor modulator (SERM), was used as the reference compound against which Fonsecinone A was compared [23]. While the docking results support the bioassay findings, they remain predictive and require further biochemical and cellular validation. Together, these data suggest that red ginger-associated endophytic fungi represent a promising yet underexplored source of bioactive metabolites with potential anticancer properties.

2. MATERIALS AND METHODS

2.1. Sample material

The materials used in this study consisted of 11 ethyl acetate extracts obtained from endophytic fungi previously isolated from red ginger (*Z. officinale* Roscoe var. *rubrum*) (Fig. 1) [18]. These extracts were selected based on prior antibacterial screening results that demonstrated their bioactivity, providing a strong rationale for evaluating their cytotoxic potential in the present work.

2.2. Brine shrimp lethality test

The BSLT assessed the toxicity of fungal extracts using hatched *Artemia salina* larvae in artificial seawater. After 48 hours of continuous aeration and light exposure at 25°C–27°C, 10 larvae were transferred to test tubes with extract concentrations ranging from 10 to 1,000 ppm. After 24 hours of exposure under temperature-controlled conditions, larval mortality was recorded [24]. The LC_{50} values were calculated using the probit method developed by Miller and Tainter and plotted manually on a log-probit graph paper, where the logarithm of concentration was plotted against the corresponding probit mortality values. LC_{50} was then determined by identifying the concentration corresponding to a probit value of 5. No statistical software was used in this analysis. This procedure was repeated three times for reliability. A control group was omitted to directly assess the cytotoxic effects of the extracts under known non-toxic solvent conditions, adhering to established protocols for such experimental setups. Incorporating control groups in future studies could enhance the validation of results, especially when testing new conditions or solvents.

2.3. Cell culture and MTT cytotoxicity assay

MCF-7 human breast cancer cells were obtained from the Cancer Chemoprevention Research Center (CCRC) at the Faculty of Pharmacy, Universitas Gadjah Mada. The cells were cultured in Dulbecco's Modified Eagle Medium (DMEM; Gibco, USA) supplemented with 10% fetal bovine serum and 1% penicillin-streptomycin, and maintained at 37°C in a humidified atmosphere containing 5% CO_2 . When the cells reached 80%–90% confluence, they were washed with phosphate-buffered saline (PBS), detached using 0.25% trypsin-ethylenediaminetetraacetic acid, and incubated for 15 minutes. The suspension was neutralized with serum-free DMEM, centrifuged at 3,000 rpm for 5 minutes, and the resulting pellet was resuspended in fresh medium. Cell viability was determined using the trypan blue exclusion method with an automated cell counter. Cells were seeded into 96-well plates at

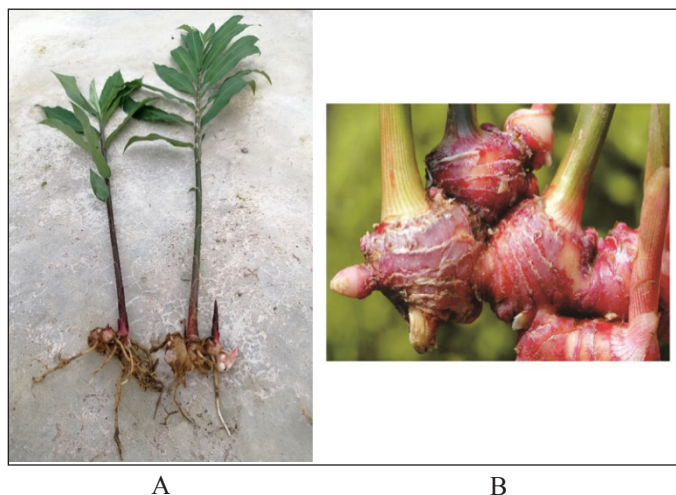


Figure 1. Red ginger plant (*Z. officinale* Roscoe var. *rubrum*): (A) stems, and (B) rhizomes.

a density of 2×10^4 cells per well in complete growth medium and incubated for 24 hours. The medium was then replaced with serum-free DMEM to synchronize the cell cycle, followed by an additional 24 hours of incubation. After synchronization, the cells were divided into three groups: treatment, untreated control, and media (blank) control.

The experimental design included treatment groups, a positive control (Paclitaxel), a cell control (untreated cells), and a media control (blank). A stock solution of the test extract (1,000 µg/ml) was prepared in dimethyl sulfoxide (DMSO) and serially diluted with DMEM to obtain final concentrations of 500, 250, 125, 62.5, and 31.25 µg/ml. Paclitaxel was tested at concentrations of 100, 50, 10, and 5 ppm. The final concentration of DMSO in all wells did not exceed 0.5% (v/v), a level generally regarded as noncytotoxic to mammalian cells. Each concentration (100 µl) was tested in triplicate and incubated for 24 hours.

After treatment, the medium was removed, the wells were washed with sterile PBS, and 25 µl of MTT solution (5 mg/ml) was added to each well. The plates were incubated at 37°C for 4 hours, after which 100 µl of DMSO was added to dissolve the formazan crystals. Absorbance was measured at 540 nm using a microplate reader, and cell viability (%) was calculated using the following equation [25]:

$$\frac{\text{OD of treatment} - \text{OD of blank}}{\text{OD of Control} - \text{OD of blank}} \times 100\%$$

The cytotoxicity of the fungal extracts was further quantified by determining the half-maximal inhibitory concentration (IC_{50}) using the same MTT assay protocol. IC_{50} values were obtained from dose-response curves by plotting the percentage of cell viability against the natural logarithm of sample concentrations ($\ln[\text{concentration}]$). Linear regression analysis was used to estimate the concentration that reduced cell viability by 50%, and IC_{50} values were also verified using probit analysis (SPSS) for improved accuracy.

2.4. Morphological and molecular characterization of endophytic fungi

Endophytic fungi were identified based on macroscopic characteristics (colony shape, colour, and edge morphology) and microscopic features. Genomic Deoxyribonucleic Acid (DNA) was extracted from selected isolates using a commercial extraction kit following the manufacturer's instructions. Polymerase chain reaction (PCR) amplification of the Internal Transcribed Spacer (ITS) region—located between conserved ribosomal RNA (rRNA) genes and widely regarded as a reliable marker for fungal identification and phylogenetic analysis—was performed using universal fungal primers ITS1 and ITS4. The thermal cycling conditions are as follows: initial denaturation at 95°C for 5 minutes, followed by 35 cycles of denaturation at 95°C for 30 seconds, annealing at 55°C for 30 seconds, and extension at 72°C for 1 minute, with a final extension at 72°C for 7 minutes. Amplified products were confirmed via electrophoresis on 1% agarose gel, purified, and subjected to Sanger sequencing. The obtained sequences were compared to reference sequences in the

National Center for Biotechnology Information GenBank database using the Basic Local Alignment Search Tool algorithm. Species-level identifications were further validated through phylogenetic tree construction using the Neighbour-Joining method with the *p*-distance model and 1,000 bootstrap replications, implemented in Molecular Evolutionary Genetics Analysis software [17,18].

2.5. Liquid chromatography–tandem mass spectrometry (LC-MS/MS) analysis of endophytic fungi extracts

The bioactive extract exhibiting significant cytotoxic activity was analyzed using LC-MS/MS to identify its secondary metabolites. The study was conducted with an XEVO G2-S quadrupole time-of-flight mass spectrometer (Waters Corp.) coupled to an Acquity Quaternary Solvent Manager system and a High Strength Silica C18 column maintained at 50°C. A 5 µl aliquot was injected and separated via gradient elution using water with ammonium formate (eluent A) and acetonitrile with formic acid (eluent B) at a 0.2 ml/min flow rate. An electrospray ionization (ESI) source was operated in positive ion mode with a capillary voltage of 3.00 kV, a desolvation temperature of 350°C, and a nitrogen gas flow rate of 739 l/h. Mass spectra were acquired in both positive and negative ionization modes. Metabolite identification was performed by comparing retention times, mass-to-charge (*m/z*) ratios, and fragmentation patterns with reference spectral databases. Data processing and compound identification were performed using MassLynx NT software (version 4.0, Waters Corp.), focusing on the $[M+H]^+$ ion species fragmented in the collision cell to produce product ions. Compound annotation relied on online databases including MassBank (<https://massbank.eu/MassBank/>), the Human Metabolome Database (HMDB, <https://www.hmdb.ca/>), and ChemSpider (<https://www.chemspider.com/>).

Fragmentation pattern matching was employed to differentiate compounds with similar *m/z* values. The MS system was operated in dual-energy mode, applying low collision energy (4 V) to detect intact precursor ions ($[M+H]^+$) and high collision energy (25–60 V) to generate fragment (daughter) ions for structural elucidation. To ensure accurate molecular mass calculations, a proton mass (1.00782 Da) was subtracted during ESI to account for protonation of the molecular ion. As authentic reference standards and nuclear magnetic resonance confirmation were not performed, all compound annotations should be regarded as tentative (putative identifications).

2.6. Molecular docking analysis

ER proteins associated with human breast cancer were selected from the Research Collaboratory for Structural Bioinformatics Protein Data Bank (<https://www.rcsb.org/>) based on crystal structures with a resolution better than 2.0 Å [26]. The structure chosen for the docking study was the ER α ligand-binding domain (PDB ID: 7KSB). For comparison, Raloxifene was selected as the standard reference ligand, as it is a clinically approved SERM widely used in the treatment of ER-positive breast cancer. The protein sequence of ER α (UniProt ID: P03372) was used for sequence alignment. The binding site was determined based on literature data and predicted using the “Site Finder” algorithm in the molecular operating environment (MOE) 2015.10 software, and subsequently validated through

the PDBsum server (<http://www.ebi.ac.uk/pdbsum>) to confirm ligand–protein interaction regions.

Protein preparation was performed using the MOE QuickPrep module with energy minimization parameters set to a root mean square (RMS) gradient of 0.01 kcal/mol/Å². The Protonate 3D tool was used to assign hydrogen atoms and optimize hydrogen bonding networks in the 3D protein structure. The ligand, Fonescinone A, was retrieved from the PubChem database (<https://pubchem.ncbi.nlm.nih.gov/>) and prepared using MOE 2015. The ligand structure was cleaned using the MOE default “Wash” function to remove unnecessary atoms and add explicit hydrogens, followed by energy minimization with an RMS gradient of 0.01 kcal/mol/Å². Drug-likeness properties of Fonescinone A were also evaluated according to Lipinski’s rule of five, which considers molecular weight (<500 Da), partition coefficient logP (<5), hydrogen bond donors (≤5), and hydrogen bond acceptors (≤10) as criteria commonly associated with oral bioavailability [20]. Molecular docking was conducted using the induced fit protocol in MOE 2015, with 100 docking runs per ligand. The best-docked conformation was selected based on binding energy and structural compatibility.

3. RESULT AND DISCUSSION

The antibacterial and cytotoxic activities of endophytic fungal extracts derived from red ginger (*Z. officinale* Roscoe var. *rubrum*) were evaluated using agar diffusion and BSLT methods, with the results summarized in Table 1. The BSLT bioassay provides a convenient and rapid preliminary indication of general toxicity but cannot directly predict cytotoxic effects in mammalian or human cells. Therefore, the LC₅₀ values obtained in this study should be regarded only as a qualitative measure of bioactivity. Further cytotoxicity testing using human cell lines is required to confirm and quantify potential human relevance.

The antibacterial potential of these extracts had already been demonstrated in our previous study [18], which reported significant inhibition against both Gram-positive and Gram-negative bacteria. Consequently, the present work emphasizes

the cytotoxic activity of the extracts against cancer cells while also re-examining their antibacterial performance.

Among the eleven extracts tested, several demonstrated notable antibacterial activity alongside varying degrees of cytotoxicity, as reflected in their LC₅₀ values. Extract JMD1 exhibited the broadest antibacterial spectrum, significantly inhibiting *Staphylococcus aureus* (8.41 ± 0.17 mm), *Escherichia coli* (11.95 ± 2.27 mm), and methicillin-resistant *Staphylococcus aureus* (MRSA) (10.60 ± 0.12 mm). It also showed moderate cytotoxicity (LC₅₀ = 377.5 ppm), suggesting its potential as a bioactive candidate for pharmaceutical development.

Extract JMB2 was active against both *S. aureus* (10.45 ± 0.13 mm) and MRSA (8.33 ± 0.24 mm), and demonstrated moderate cytotoxicity with an LC₅₀ value of 116.7 ppm. Its dual antibacterial activity, particularly against drug-resistant MRSA, highlights its therapeutic potential, although the cytotoxicity profile requires careful evaluation in subsequent studies. Similarly, JMB1 inhibited *S. aureus* (8.33 ± 0.24 mm) and exhibited an LC₅₀ of 100 ppm, placing it within the moderately toxic range. Although its antibacterial spectrum was narrower, its selectivity and balanced toxicity profile make it a noteworthy extract for further investigation. Among the active extracts, ZOB5 was distinguished by its low toxicity (LC₅₀ = 1,052.8 ppm), the highest among all samples, while exhibiting antibacterial activity against *S. aureus* (7.55 ± 0.33 mm). Although its antimicrobial potency was limited, its high biocompatibility suggests potential applications in topical formulations or food preservation.

Notably, ZOBT1 exhibited selective antibacterial activity against *E. coli* (8.44 ± 0.30 mm) and displayed an LC₅₀ value of 89.4 ppm in the BSLT assay. While its antibacterial spectrum was narrow, its effectiveness against *E. coli*, a Gram-negative bacterium often resistant to natural compounds, and its relatively low toxicity highlight its promise as a novel antibacterial candidate [27].

Based on these results, subsequent investigations focused on ZOBT1, including cytotoxicity testing against MCF-7 cells, chemical profiling via LC-MS/MS, and molecular

Table 1. Antibacterial activity and toxicity screening (BSLT) of endophytic fungal extracts from red ginger plant (*Z. officinale* var. *rubrum*).

No	Code of extract	Zone of inhibition ± Standard deviation (SD) in mm			LC ₅₀ (ppm)
		<i>S. aureus</i>	<i>E. coli</i>	MRSA	
1	ZOBT1	-	8.44 ± 0.30	-	89.4
2	ZOB1	-	-	-	72.8
3	ZOB2	-	-	-	1.6
4	ZOB5	7.55 ± 0.33	-	-	1,052.8
5	ZOB6	-	-	-	46.8
6	ZOB7	-	-	-	193.3
7	JMR3	-	-	-	37.9
8	JMB1	8.33 ± 0.24	-	-	100
9	JMB2	10.45 ± 0.13	-	8.33 ± 0.24	116.7
10	JMD1	8.41 ± 0.17	11.95 ± 2.27	10.60 ± 0.12	377.5
11	JMD2	-	-	9.55 ± 0.15	151.5

docking of its active compounds to target proteins. In summary, extracts JMD1, JMB2, and ZOBT1 emerged as promising candidates due to their antibacterial efficacy and acceptable cytotoxicity. Among these, ZOBT1's selective potency against Gram-negative bacteria positions it as a compelling source for developing novel antibacterial agents [28].

Figure 2 presents the macroscopic (A) and microscopic (B) characteristics of the endophytic fungal isolate ZOBT1, derived from red ginger (*Z. officinale* var. *rubrum*). In the macroscopic view (Fig. 2A), the colony morphology of ZOBT1 on Sabouraud Dextrose Agar is shown, exhibiting rapid growth with a dark brown to black pigmentation, white margins, and a rough, fibrous surface texture. The microscopic image (Fig. 2B) reveals the microstructural features of ZOBT1, including septate hyphae and biserial conidiophores bearing conidia. The conidiophores are cylindrical, round, and biserial, measuring approximately 200–400 μm long and 7–10 μm in diameter. The conidia are dark brown to blackish, with smooth to rough surfaces, measuring 30–75 μm in length and 2.5–4 μm in diameter. These morphological characteristics support the preliminary identification of the fungal isolate and provide a foundation for further taxonomic or molecular analysis [25].

PCR amplification results for molecular identification of the ZOBT1 isolate are presented in Figure 3, visualized using agarose gel electrophoresis. A single, clear DNA band of approximately 430 bp was observed in Lanes 1 (ZOBT1), indicating successful and specific amplification. In contrast, no band appeared in the no-template control (NTC), confirming the absence of contamination. Figure 4 presents a phylogenetic tree illustrating the evolutionary relationship between isolate ZOBT1 and several closely related fungal species based on 18S rRNA gene sequence analysis. The tree was constructed using the neighbor-joining method, and bootstrap values (shown at branch nodes) represent the confidence level of each clustering relationship. The sequence data of the ZOBT1 isolate were submitted to GenBank with accession number PX671564.

The isolate ZOBT1 clusters closely with the *Aspergillus niger* strain MM1 (MH091025.1), exhibiting a high bootstrap value of 98%, indicating substantial genetic similarity. ZOBT1 also shares a close evolutionary relationship with other *Aspergillus* species, including *Aspergillus* sp. MR55 (KT374059.1) and *Aspergillus welwitschiae* isolate SD2005S36a (PX091645.1), supported by bootstrap values of

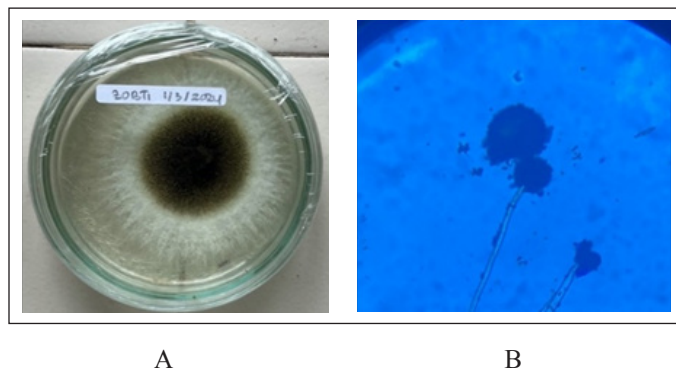


Figure 2. Macroscopic (A) and microscopic (B) pictures of fungal isolate ZOBT1.

82% and 87%, respectively. In contrast, *Alternaria alternata* (MT994282.1) and *Penicillium* species (*P. oxalicum* and *P. sclerotigenum*) form distinct branches with lower similarity, indicating that ZOBT1 is phylogenetically more related to members of the *Aspergillus* genus. Overall, the phylogenetic analysis confirms that isolate ZOBT1 belongs to the *Aspergillus* clade, with its closest affiliation to *A. niger* strain MM1, suggesting that ZOBT1 is either a strain or a closely related variant of *A. niger*.

The cytotoxic effect of the endophytic fungal extract derived from *A. niger* ZOBT1 was evaluated on MCF-7 human breast cancer cells using the MTT assay. The cell line was

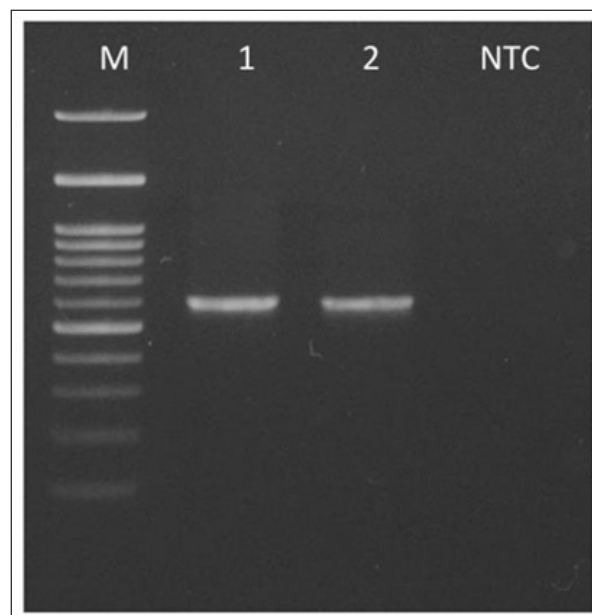


Figure 3. Agarose gel electrophoresis showing PCR amplification of the target DNA fragment. Lane M: 100 bp DNA marker; Lanes 1 (ZOBT1): specific PCR products of approximately 430 bp; Lane NTC: negative control (no amplification observed).

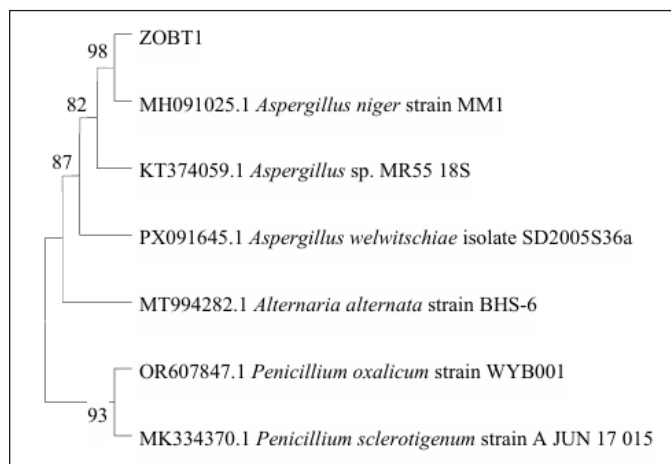


Figure 4. Using the neighbor-joining algorithm and 1,000 bootstraps, the concatenated phylogenetic tree of isolate ZOBT1 with *A. niger* strain OR32F, based on ITS and large subunit (LSU) rDNA region sequences.

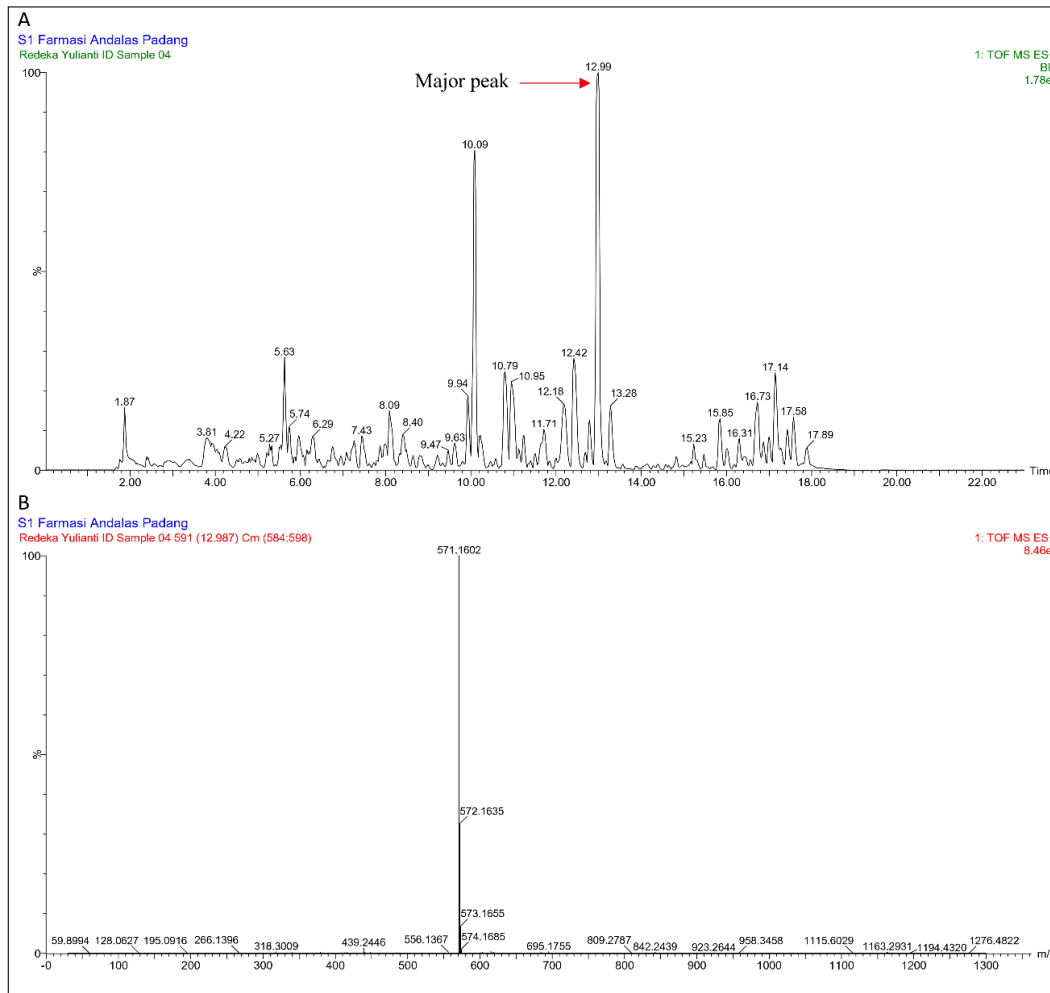


Figure 5. LC-MS/MS chromatogram ZOBT1 extract (A), and the major peak was observed at a retention time of 12.99 minutes using ESI in positive mode (B).

Table 2. Chemical composition of the ethyl acetate extract from the endophytic fungus *A. niger* ZOBT1, identified by LC-MS/MS in positive ion mode, including compound names, retention times, and peak intensities.

Extract	RT (min)	Parent ion (m/z)	Molecular formula	Tentative identification
ZOBT1	5.63	224.0566	C ₁₀ H ₉ NO ₅	Pyranonigrin A
	5.96	229.0875	C ₁₁ H ₁₆ O ₅	2-Methylidene-3-(5-oxohexyl)butanedioic acid
	6.44	273.1247	C ₁₆ H ₁₆ O ₄	2-(2-Hydroxyphenyl) acetic acid 4-hydroxyphenethyl ester
	6.75	185.0458	C ₈ H ₈ O ₅	Spinulosin
	6.95	196.0618	C ₉ H ₉ NO ₄	4-Hydroxyphenyl pyruvic acid oxime
	9.94	456.1662	C ₂₃ H ₂₅ N ₃ O ₇	Perquinoline B
	10.09	457.1763	C ₂₇ H ₂₄ N ₂ O ₅	Aspernigrin B
	10.22	472.1761	C ₂₇ H ₂₅ N ₃ O ₅	Clavatustide A
	10.95	530.2484	C ₂₃ H ₃₉ N ₅ O ₅ S ₂	Malformin A
	12.42	571.1615	C ₃₂ H ₂₆ O ₁₀	Aurasperone A
	12.99	571.1602	C ₃₂ H ₂₆ O ₁₀	Fonsecinone A
	15.23	586.3168	C ₃₇ H ₄₇ NO ₅	Secopenitrem B
	15.47	588.3323	C ₃₂ H ₃₃ N ₃ O ₈	Versicoamide H

Note: All compounds are reported as putative identifications based on LC-MS/MS database matching. Structural confirmation with authentic standards and NMR is required.

obtained from the CCRC Laboratory at the Faculty of Pharmacy, Universitas Gadjah Mada. The MTT assay was employed as a standard method for assessing cell viability. In this assay, the yellow MTT compound is reduced by mitochondrial enzymes in viable cells to form purple formazan crystals. The intensity of the purple coloration is directly proportional to the number of metabolically active cells, thereby allowing the cytotoxic potential of the extract to be quantitatively determined.

The fungal extract was tested at five concentrations: 500, 250, 125, 62.5, and 31.25 $\mu\text{g/ml}$, with each level tested in triplicate. This range was chosen to help pinpoint the lowest effective dose and to calculate the IC_{50} , the concentration needed to reduce cancer cell growth by 50%. A dose-response curve was created by plotting the log of each concentration against the percentage of surviving cells, and the IC_{50} was calculated using linear regression.

According to standards from the National Cancer Institute and guidelines by Niksic *et al.* [29], compounds are classified as highly cytotoxic if their IC_{50} is 20 $\mu\text{g/ml}$ or lower, moderately cytotoxic between 21 and 200 $\mu\text{g/ml}$, weakly cytotoxic between 201 and 500 $\mu\text{g/ml}$, and inactive if above 500 $\mu\text{g/ml}$. The *A. niger* ZOBT1 extract demonstrated potent cytotoxicity with an IC_{50} value of 20.10 $\mu\text{g/ml}$, placing it near the threshold of the highly cytotoxic classification. This level of activity indicates substantial inhibitory potential against MCF-7 breast cancer cells. For comparison, the reference drug Paclitaxel showed a stronger effect, with an IC_{50} of 11.09 $\mu\text{g/ml}$ [29].

The extract of *A. niger* ZOBT1 was analyzed using LC-MS/MS equipped with an ultra-performance liquid chromatography–quadrupole time-of-flight mass spectrometer (UPLC-QTOF-MS/MS). This high-resolution analytical technique was employed to identify bioactive secondary metabolites potentially responsible for the extract's cytotoxic activity. The sensitivity and mass accuracy of UPLC-QTOF-MS/MS enable precise detection and structural characterization of various compound classes, including phenolics, flavonoids, alkaloids, and terpenoids, many of which are associated with anticancer properties.

Chromatographic separation was performed using a C18/octadecylsilane (ODS) column, selected for its strong retention of hydrophobic analytes and compatibility with aqueous-rich mobile phases. The mobile phase consisted of two eluents: eluent A (ultrapure water [aquabidest] with 0.1% formic acid, v/v) and eluent B (acetonitrile with 0.1% formic acid, v/v). A gradient elution protocol was employed with a flow rate of 0.2 ml/min over a total runtime of 22 minutes. This solvent system was optimized to enhance solubility, improve peak resolution, and protect the stationary phase from degradation, facilitating efficient separation of polar and nonpolar compounds.

Mass spectrometry data were acquired and processed using MassLynx™ software, which generated chromatograms and MS spectra for molecular weight determination and formula prediction. Compound identification was achieved by matching the observed molecular formulas and fragmentation patterns with those available in public MS databases, including MassBank, the HMDB, and ChemSpider. To ensure accurate compound annotation, MS/MS spectra were compared

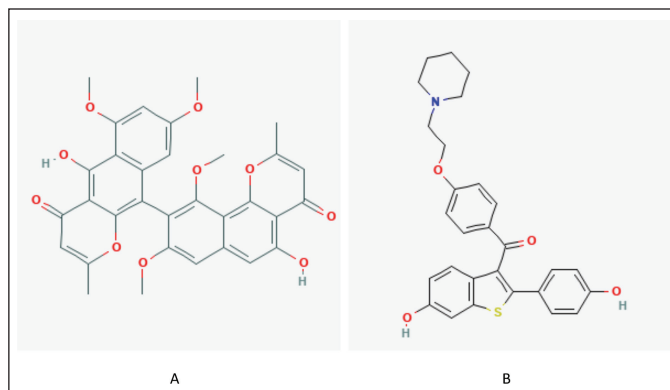


Figure 6. Chemical structures of (A) Fonsecinone A, a benzophenone derivative identified as the major metabolite in the *A. niger* ZOBT1 extract, and (B) Raloxifene, a clinically approved SERM used here as the standard reference compound for docking studies.

with reference fragmentation data, taking into account that isobaric compounds may share similar m/z values but differ in fragmentation behavior.

The results of the LC–MS/MS analysis of the ZOBT1 extract, including the chromatogram and the corresponding mass spectra of each detected peak, are shown in Figure 5 and summarized in Table 2. LC–MS/MS profiling of the *A. niger* ZOBT1 extract identified thirteen distinct compounds (Fig. 5A). These compounds were tentatively annotated by comparing their MS/MS fragmentation patterns and accurate mass values with reference data from PubChem, ChemSpider, and MassBank databases, and are listed in Table 2 as putative identifications. The major peak observed at a retention time of 12.99 minutes corresponded to Fonsecinone A (m/z 571.1602), identified as the predominant metabolite in the ZOBT1 extract (Fig. 5B).

Fonsecinone A (Fig. 6A), a benzophenone derivative, has been reported to exhibit a range of biological activities, including cytotoxic and antimicrobial effects. Its prominence in the extract supports its possible contribution to the observed cytotoxic activity against MCF-7 breast cancer cells, although mechanistic studies are required for confirmation. The findings emphasize the critical role of LC-MS/MS in comprehensive metabolite profiling, enabling the detection of bioactive constituents and providing insights into potential synergistic effects [30]. Collectively, these results provide a biochemical basis for the subsequent molecular docking study of Fonsecinone A.

Fonsecinone A was subsequently selected for molecular docking analysis because it was detected as the major peak in the chromatogram, indicating that it is the most abundant compound in the extract. Previous studies have also reported its cytotoxic and antimicrobial activities, supporting its plausibility as a key contributor to the observed bioactivity [30]. Therefore, focusing on the predominant compound was considered a rational approach for this preliminary docking evaluation, while acknowledging that future studies should expand the analysis to additional metabolites to provide a more comprehensive understanding.

Table 3. Result of molecular docking fonsecinone A and raloxifene (Reference ligand).

No	Compound	S score (kcal/mol)	RMSD_refine (Å)	Hydrogen bond	Carbon-hydrogen bond	Van der Waals interaction	Amino acid residue (hydrogen bond)
1	Raloxifene (Reference ligand)	-7.3585	2.3388	2	3	9	Trp393, Glu397
2	Fonsecinone A	-5.3536	1.7373	1	5	7	Trp393

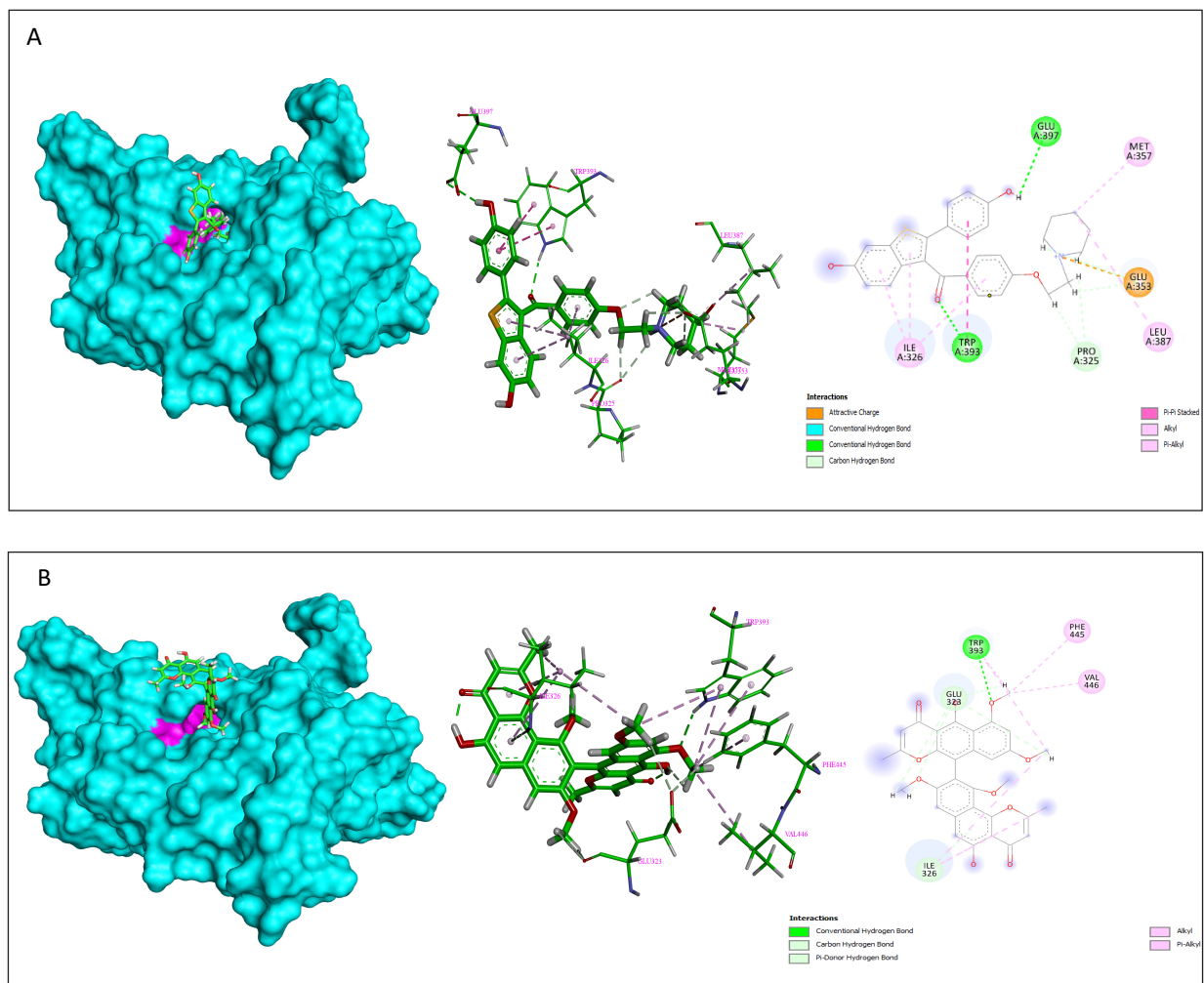


Figure 7. (A) Docked conformation of raloxifene in the active site of ER α ligand-binding domain (PDB ID: 7KSB). (B) Docked conformation of fonsecinone A in the same active site. Protein surface is shown in cyan; key binding-site residues (Glu353, Arg394, His524, Tyr537, Asp538, and Trp393) are highlighted in magenta. Ligands are rendered in stick representation (CPK coloring). The right panels show 2D interaction diagrams, detailing hydrogen bonds, π -interactions, electrostatic interactions, and hydrophobic contacts.

Although only Fonsecinone A was tested *in silico*, the crude extract contains multiple metabolites that may act synergistically or antagonistically. For instance, combinations of phenolic compounds, such as gallic acid and caffeic acid, exhibit significant synergistic antioxidant effects (increased by 137.8%), whereas certain ternary combinations may result in antagonistic interactions [31]. This limitation underscores the importance of future studies involving multitarget docking or combinatorial bioassays to identify potential interactions among metabolites.

Several intrinsic and extrinsic factors highly influence the production of bioactive metabolites by endophytic fungi.

At the strain level, genetic variability among endophytes can result in distinct biosynthetic capabilities, leading to differences in metabolite profiles even among isolates derived from the same host plant. Host plant species and tissue type also play a crucial role, as the endophyte host interaction often regulates the expression of secondary metabolites. Additionally, environmental factors such as geographical location, soil composition, and climate conditions can further influence the endophytic community structure and metabolic output. During laboratory cultivation, the composition of the culture medium, pH, incubation time, and aeration are critical parameters that can significantly alter metabolite yield and diversity. Such

variability underscores the importance of standardizing isolation and fermentation conditions while exploring multiple strains to identify robust producers. Recognizing these factors provides valuable context for understanding the variability in biological activities observed in this study and highlights opportunities for optimizing metabolite production in future investigations [32,33]. This variability explains why two isolates of the same fungal species may produce distinct sets or quantities of secondary metabolites. Addressing this point clarifies that the observed biological activity of *A. niger* ZOB1 is not universal for all *A. niger*, but may be specific to the strain–host–environment interaction.

Raloxifene, a well-established SERM, was used as a reference compound to validate the molecular docking approach in this study. It is known to exert antagonistic effects on ER α in breast tissue while acting as an agonist in bone, making it a clinically relevant model for anti-estrogenic activity. In the present analysis, Raloxifene exhibited a binding score of -7.3585 kcal/mol and a root mean square deviation_refine (RMSD_refine) value of 2.3388 Å, consistent with its strong affinity and stable binding at the canonical ER α pocket. Its interactions, involving key residues such as Glu353, Arg394, and His524, served as a benchmark for assessing the binding characteristics of Fonsecinone A. Consequently, Raloxifene's performance provided a reliable comparative standard, allowing evaluation of the relative binding stability and interaction diversity of the fungal-derived compound toward ER α .

As shown in Table 3, Raloxifene exhibited a binding score of -7.3585 kcal/mol, while Fonsecinone A showed a slightly lower score of -5.3536 kcal/mol. Nevertheless, Fonsecinone A exhibited richer interaction patterns, including Van der Waals and carbon-hydrogen interactions, and notably engaged additional residues such as Tyr537, Asp538, and Trp393 (Fig. 7). Although Trp393 is not classically part of the canonical binding site, its aromatic nature suggests potential π – π stacking interactions, which have been implicated in ligand stabilization in other receptor systems. Its engagement by Fonsecinone A suggests potential relevance in modulating receptor activity or ligand orientation. Furthermore, Fonsecinone A exhibited a lower RMSD_refine value (1.7373 Å) compared to Raloxifene (2.3388 Å), suggesting a more stable docking pose with less deviation during refinement [34,35]. While Raloxifene maintains superior predicted affinity, Fonsecinone A interacted with additional residues such as Tyr537, Asp538, and Trp393, and adopted a relatively stable binding pose with a lower RMSD_refine value. These results provide preliminary *in silico* indications that Fonsecinone A may interact with ER α in a distinct binding orientation. However, given its weaker binding score compared to Raloxifene and the absence of re-docking validation, competitive binding assays, or reporter gene assays, these findings remain hypothetical and should not be overinterpreted.

Fonsecinone- and aurasperone-type naphtho- γ -pyrones are known fungal metabolites with reported cytotoxic and antioxidant activities. In this work, their detection in *A. niger* ZOB1 represents an additional occurrence within a different fungal host, rather than the discovery of new chemical entities. The study provides confirmatory and comparative evidence of

their cytotoxic potential, supported by *in silico* docking results and bioassay data, thereby expanding the chemotaxonomic and biological context of this compound class [36–38].

This study has several limitations, including its restriction to *in vitro* and *in silico* analyses, the use of only one breast cancer cell line (MCF-7), and the focus on a single molecular target (ER α). These factors limit the generalizability of the findings and highlight the need for *in vivo* validation and expansion to other cancer models and pathways. Nonetheless, identifying Fonsecinone A as a major metabolite with antimicrobial and cytotoxic activities underscores the potential of endophytic fungi from red ginger as a source of bioactive compounds. The observed selective activity against drug-resistant bacteria, along with its distinct interactions with ER α , suggests important clinical implications. Future research should therefore validate these results *in vivo*, explore additional cell lines and molecular targets, and investigate the synergistic or antagonistic effects of other metabolites to assess their therapeutic value fully.

4. CONCLUSION

This study provides preliminary evidence of the cytotoxic and ER-binding potential of the endophytic fungus *A. niger* ZOB1 isolated from *Z. officinale* var. rubrum (red ginger). The fungal extract exhibited cytotoxic effects against MCF-7 breast cancer cells, and LC-MS/MS analysis identified Fonsecinone A as a major active compound likely contributing to this activity. Although its docking score against ER α was lower than that of the reference drug Raloxifene, Fonsecinone A engaged critical residues, such as Trp393, also targeted by Raloxifene, and exhibited a more stable binding conformation, as reflected by its lower RMSD_refine value. These findings suggest that while both compounds share similar interaction sites, Fonsecinone A may adopt a distinct and stable binding mode, reinforcing its potential as a novel anticancer lead compound. Nevertheless, the study is limited to a single cancer cell line and one molecular target; further *in vivo* studies, alongside the isolation of pure compounds, are warranted to validate and expand these results.

5. ACKNOWLEDGMENT

Financial support was gratefully received from Andalas University, Padang, Indonesia, for the project entitled Penelitian Dasar Unggulan Klaster Riset Publikasi Guru Besar (PDU-KRP1GB-Unand), under Grant No. T/6/UN.16.17/PT.01.03/KO-PDUKRP1GB-Unand/2022.

6. AUTHORS' CONTRIBUTIONS

All authors made substantial contributions to conception and design, acquisition of data, or analysis and interpretation of data; took part in drafting the article or revising it critically for important intellectual content; agreed to submit to the current journal; gave final approval of the version to be published; and agree to be accountable for all aspects of the work. All the authors are eligible to be author as per the International Committee of Medical Journal Editors (ICMJE) requirements/guidelines.

7. CONFLICTS OF INTEREST

The authors report no financial or any other conflicts of interest in this work.

8. ETHICAL APPROVAL

This study involved brine shrimp larvae (*Artemia salina*) for preliminary toxicity screening and established human-derived cell lines (MCF-7) for cytotoxicity assays. No experiments involving vertebrate animals or human participants were conducted.

9. DATA AVAILABILITY

All data collected and analyzed in this study have been included in the present article.

10. PUBLISHER'S NOTE

All claims expressed in this article are solely those of the authors and do not necessarily represent those of the publisher, the editors and the reviewers. This journal remains neutral with regard to jurisdictional claims in published institutional affiliation.

11. USE OF ARTIFICIAL INTELLIGENCE (AI)-ASSISTED TECHNOLOGY

The authors declare that they have not used artificial intelligence (AI)-tools for writing and editing of the manuscript, and no images were manipulated using AI.

REFERENCES

- Bray F, Laversanne M, Sung H, Ferlay J, Siegel RL, Soerjomataram I, *et al.* Global cancer statistics 2022: GLOBOCAN estimates of incidence and mortality worldwide for 36 cancers in 185 countries. *CA Cancer J Clin.* 2024;74(3):229–63. doi: <https://doi.org/10.3322/caac.21834>
- Kumar A, Singh K, Kumar K, Singh A, Tripathi A, Tiwari L. Drug resistance in cancer therapy: mechanisms, challenges, and strategies. *Asian J Nurs Educ Res.* 2024;14(1):95–100. doi: <https://doi.org/10.52711/2349-2996.2024.00019>. Available from: <https://ajner.com/AbstractView.aspx?PID=2024-14-1-19>
- Kulkarni P, Mohanty A, Bhattacharya S, Singhal S, Guo L, Ramisetty S, *et al.* Addressing drug resistance in cancer: a team medicine approach. *J Clin Med.* 2022;11(19):5701. doi: <https://doi.org/10.3390/jcm11195701>
- Gallagher K, Martin MY, Angove RSM. The tipping point: financial and emotional costs of care for medicare patients with cancer. *JCO Oncol Pract.* 2024;20(10):260. doi: https://doi.org/10.1200/OP.2024.20.10_suppl.260
- Esmeta A, Adhikary S, Dharshna V, Swarnamughi P, Ummul Maqsummiya Z, Radhakrishnan R, *et al.* Plant-derived bioactive compounds in colon cancer treatment: an updated review. *Biomed Pharmacother.* 2022;153:113384. doi: <https://doi.org/10.1016/j.biopha.2022.113384>
- Satriawan H, Zaimi NA, Eriadi A, Efdi M, Tallei TE, Andayani R, *et al.* Isolation and evaluation of the antimicrobial activity of endophytic fungi from *Orthosiphon aristatus*. *Biodiversitas.* 2025;26(2):963–70. doi: <https://doi.org/10.13057/biodiv/d260225>
- Nuraini P, Wicaksono DP, Laosuwan K, Putri AA. The effect of red ginger essential oil on adherence of *Streptococcus mutans*. *J Pure Appl Microbiol.* 2024;18(1):542–8. doi: <https://doi.org/10.22207/JPAM.18.1.58>
- Hendra RJ, Rusdi R, Asra R, Misfadhila S. Phytochemical and traditional uses of red ginger: a review (*Zingiber officinale* var. *rubrum*). *EAS J Pharm Pharmacol.* 2022;4(3):50–5. doi: <https://doi.org/10.36349/easjpp.2022.v04i03.001>
- Dari S, Azizah Z, Chandra B. Phytochemical and pharmacological review of red ginger extracts (*Zingiber officinale* var. *rubrum*). *IOSR J Pharm Biol Sci.* 2022;17(1):1–6. doi: <https://doi.org/10.9790/3008-1701042430>. Available from: www.iosrjournals.org
- Wallace D. Natural products as a source of anticancer lead compounds: ginger and breast cancer. *J Pharmacol Clin Res.* 2016;1(3):1–3. doi: <https://doi.org/10.19080/JPCR.2016.01.555564>
- Morales-Vargas AT, López-Ramírez V, Álvarez-Mejía C, Vázquez-Martínez J. Endophytic fungi for crops adaptation to abiotic stresses. *Microorganisms.* 2024;12(7):1357. doi: <https://doi.org/10.3390/microorganisms12071357>
- Collinge DB, Jensen B, Jørgensen HJ. Fungal endophytes in plants and their relationship to plant disease. *Curr Opin Microbiol.* 2022;69:102177. doi: <https://doi.org/10.1016/j.mib.2022.102177>
- Powar PV, Chaudhari S. Unexploited potentials of endophytic fungi: patents review on endophytic fungi related to secondary bioactive compounds. *Pharmacogn Res.* 2023;15(2):217–25. doi: <https://doi.org/10.5530/pr.2023.2.34>
- Torres-Mendoza D, Ortega HE, Cubilla-Rios L. Patents on endophytic fungi related to secondary metabolites and biotransformation applications. *J Fungi.* 2020;6(2):58. doi: <https://doi.org/10.3390/jof6020058>
- El-Zehery HRA, Ashry NM, Faiesal AA, Attia MS, Abdel-Maksoud MA, *et al.* Antibacterial and anticancer potential of bioactive compounds and secondary metabolites of endophytic fungi isolated from *Anethum graveolens*. *Front Microbiol.* 2024;15:1448191. doi: <https://doi.org/10.3389/fmicb.2024.1448191>
- Kaliaperumal K, Salendra L, Liu Y, Ju Z, Sahu SK, *et al.* Isolation of anticancer bioactive secondary metabolites from the sponge-derived endophytic fungi *Penicillium* sp. and *in-silico* computational docking approach. *Front Microbiol.* 2023;14:1216928. doi: <https://doi.org/10.3389/fmicb.2023.1216928>
- Sandrawati N, Hati SP, Yunita F, Putra AE, Ismed F, Tallei TE, *et al.* Antimicrobial and cytotoxic activities of marine sponge-derived fungal extracts isolated from *Dactylosporgia* sp. *J Appl Pharm Sci.* 2020;10(4):28–33. doi: <https://doi.org/10.7324/JAPS.2020.104005>
- Handayani D, Sari HC, Julianti E, Artasasta MA. Endophytic fungus isolated from *Zingiber officinale* Linn. var. *rubrum* as a source of antimicrobial compounds. *J Appl Pharm Sci.* 2023;13(9):115–20. doi: <http://dx.doi.org/10.7324/JAPS.2023.134154>
- Hopkinson BM, Klitgaard MC, Petersen OW, Villadsen R, Rønnow-Jessen L, Kim J. Establishment of a normal-derived estrogen receptor-positive cell line comparable to the prevailing human breast cancer subtype. *Oncotarget.* 2017;8(6):10580–94. doi: <https://doi.org/10.18632/oncotarget.14157>
- Handayani D, Aminah I, Pontana Putra P, Eka Putra A, Arbain D, Satriawan H, *et al.* The depsidones from marine sponge-derived fungus *Aspergillus unguis* IB151 as an anti-MRSA agent: molecular docking, pharmacokinetics analysis, and molecular dynamic simulation studies. *Saudi Pharm J.* 2023;31(9):101744. doi: <https://doi.org/10.1016/j.jsps.2023.101744>
- Ismail NZ, Md Toha Z, Muhammad M, Nik Mohamed Kamal NNS, Mohamad Zain NN, Arsad H. Antioxidant effects, antiproliferative effects, and molecular docking of *Clinacanthus nutans* leaf extracts. *Molecules.* 2020;25(9):2067. doi: <https://doi.org/10.3390/molecules25092067>
- Artasasta MA, Yanwirasti Y, Taher M, Djamaan A, Ariantari NP, Edrada-Ebel RA, *et al.* Apoptotic activity of new oxisterigmatocystin derivatives from the marine-derived fungus *Aspergillus nomius* nc06. *Mar Drugs.* 2021;19(11):631. doi: <https://doi.org/10.3390/md19110631>
- O'Malley A, Pote S, Giangrieco I, Tuppo L, Gawlicka-Chruszcz A, Kowal K, *et al.* Structural characterization of Act c 10.0101 and Pun g 1.0101—Allergens from the non-specific lipid transfer protein family. *Molecules.* 2021;26(2):256. doi: <https://doi.org/10.3390/molecules26020256>

24. Meyer B, Ferrigni N, Putnam J, Jacobsen L, Nichols D, McLaughlin J. Brine shrimp: a convenient general bioassay for active plant constituents. *Planta Med.* 1982;45(5):31–4. doi: <https://doi.org/10.1055/s-2007-971297>
25. Handayani D, Rasyid W, Rustini, Zainudin EN, Hertiani T. Cytotoxic activity screening of fungal extracts derived from the West Sumatran marine sponge *Haliclona fascigera* to several human cell lines: heLa, WiDr, T47D and Vero. *J Appl Pharm Sci.* 2018;8(1):55–8. doi: <https://doi.org/10.7324/JAPS.2018.8108>
26. Khelfaoui H, Harkati D, Saleh BA. Molecular docking, molecular dynamics simulations and reactivity studies on approved drugs library targeting ACE2 and SARS-CoV-2 binding with ACE2. *J Biomol Struct Dyn.* 2021;39(18):7246–62. doi: <https://doi.org/10.1080/07391102.2020.1850352>
27. Seyedalinaghi S, Mehraeen E, Mirzapour P, Yarmohammadi S, Dehghani S, Zare S, *et al.* A systematic review on natural products with antimicrobial potential against WHO's priority pathogens. *Eur J Med Res.* 2025;30(1):1–2. doi: <https://doi.org/10.1186/s40001-025-02717-x>
28. Hamad M, Al-Marzooq F, Srinivasulu V, Sulaiman A, Menon V, Ramadan WS, *et al.* Antimicrobial activity of nature-inspired molecules against multidrug-resistant bacteria. *Front Microbiol.* 2023;14:1336856. doi: <https://doi.org/10.3389/fmicb.2023.1336856>
29. Niksic H, Becic F, Koric E, Gusic I, Omeragic E, Muratovic S, *et al.* Cytotoxicity screening of *Thymus vulgaris* L. essential oil in brine shrimp nauplii and cancer cell lines. *Sci Rep.* 2021;11:21938. doi: <https://doi.org/10.1038/s41598-021-92679-x>
30. Zhang P, Liu H, Yu Y, Peng S, Zeng A, Song L. Terpenoids mediated cell apoptosis in cervical cancer: mechanisms, advances and prospects. *Fitoterapia.* 2025;180:106323. doi: <https://doi.org/10.1016/j.fitote.2024.106323>
31. Khazaaal HT, Khazaaal MT, Abdel-Razek AS, Hamed AA, Ebrahim HY, Ibrahim RR, *et al.* Antimicrobial, antiproliferative activities and molecular docking of metabolites from *Alternaria alternata*. *AMB Express.* 2023;13(1):19. doi: <https://doi.org/10.1186/s13568-023-01568-1>
32. Boța M, Vlaia L, Jijie AR, Marcovici I, Crișan F, Oancea C, *et al.* Exploring synergistic interactions between natural compounds and conventional chemotherapeutic drugs in preclinical models of lung cancer. *Pharmaceuticals.* 2024;17(5):598. doi: <https://doi.org/10.3390/ph17050598>
33. El-Sayed ESR, Kloc M, Kulbacka J, Choromańska A, Bielecka M, Strzala T, *et al.* Bioprospecting endophytic fungi of forest plants for bioactive metabolites with anticancer potentials. *Sci Rep.* 2025;15:10372. doi: <https://doi.org/10.1038/s41598-025-10372-9>
34. Satriawan H, Teoh TC, Rizman-Idid M, Krishnan A, Bakar NA, Alias SA, *et al.* Polar fungi *Pseudogymnoascus*: secondary metabolites and ecological significance. *Chiang Mai J Sci.* 2024;51(3):537–52. doi: <https://doi.org/10.12982/CMJS.2024.043>
35. Palaniveloo K, Ong KH, Satriawan H, Abdul Razak S, Suciati S, Hung HY, *et al.* *In vitro* and *in silico* cholinesterase inhibitory potential of metabolites from *Laurencia snackeyi* (Weber-van Bosse) M. Masuda. *3 Biotech.* 2023;13(10):375. doi: <https://doi.org/10.1007/s13205-023-03725-6>
36. Zainul R, Verawati R, Satriawan H, Wargasetia TL, Purnamasari D, Lubis AP, *et al.* Molecular docking of theaflavin from *Camellia sinensis* in inhibiting B-cell lymphoma through BCL2 apoptosis regulator: an *in silico* study. *Pharmacogn J.* 2023;15(4):500–5. doi: <https://doi.org/10.5530/pj.2023.15.85>
37. Deshmukh SK, Verekar SA. Fungal endophytes: a potential source of antifungal compounds. *Front Biosci.* 2012;4:2045–70. doi: <https://doi.org/10.2741/523>
38. Orfali R, Aboseada MA, Abdel-Wahab NM, Hassan HM, Perveen S, Ameen F, *et al.* Recent updates on the bioactive compounds of the marine-derived genus *Aspergillus*. *RSC Adv.* 2021;11(28):17116–50. doi: <https://doi.org/10.1039/D1RA01359A>

How to cite this article:

Satriawan H, Ulinza P, Kuo P-C, Handayani D. Cytotoxic activity and potential estrogen receptor interactions of extracts from red ginger endophytic fungus *Aspergillus niger* ZOBT1. *J Appl Pharm Sci.* 2026;16(04):125-135. DOI: 10.7324/JAPS.2026.269547